LETTER

Infrared SPR sensitivity enhancement using ITO/TiO_2/silicon overlays

To cite this article: A. K. Mishra and S. K. Mishra 2015 *EPL* **112** 10001

A Letters Journal Exploring the Frontiers of Physics

October 2015

EPL, **112** (2015) 10001 www.epljournal.org
doi: 10.1209/0295-5075/112/10001

Infrared SPR sensitivity enhancement using ITO/TiO_2/silicon overlays

A. K. Mishra[1(a)] and S. K. Mishra[2]

[1] *Department of Electrical Engineering, Technion-Israel Institute of Technology - Haifa-32000, Israel*
[2] *Electronic Engineering Department, City University of Hong Kong - Tat Chee Avenue, Hong Kong*

received 17 August 2015; accepted in final form 23 September 2015
published online 12 October 2015

PACS 07.07.Df – Sensors (chemical, optical, electrical, movement, gas, etc.); remote sensing
PACS 42.81.Pa – Sensors, gyros

Abstract – An extremely high sensitive surface-plasmon-resonance–based fiber optic sensing probe working in the infrared region of electromagnetic spectrum has been proposed and characterized theoretically. The optimized fiber probe is designed by coating 40 nm of indium tin oxide (ITO), 9 nm of titanium dioxide (TiO_2) and a field enhancing 26 nm of silicon layers on a multimode bare fiber core. The probe is characterized for refractive index range of 1.33 to 1.37 refractive index unit (RIU). The highest sensitivity and figure of merit for optimized probe design parameters are found to be 15.07 μm/RIU and 18.962 RIU^{-1}, respectively at sensing medium refractive index 1.37 RIU.

Introduction. – Surface plasmon resonance (SPR) enabled with its tremendous capability of confining light in the sub-wavelength dimension has found applications ranging from imaging to sensing. A wide range of lithographically designed structured materials such as nanoantennas [1] and metamaterials [2,3] are exploiting this deeper confinement properties to their most.

SPR excites at the interface of two materials having opposite signs of the real part of their permittivities and decays evanescently in both of these materials. Since the evanescent tail of SPR is very sensitive to any change in the permittivity of the surrounding medium, one of the most extensive areas of application of the SPR phenomenon is in the refractive index sensing. Two configurations, the Otto and Kretschmann ones, have been proposed to realise the SPR-based sensors experimentally. Additionally, there are two methods of interrogation in both of these configurations —wavelength interrogation and angular interrogation. In the wavelength interrogation method, the angle of incidence of the incident light is kept fixed and the wavelength is varied continuously to meet the condition of the phase matching for the excitement of the surface plasmon wave (SPW) at the desired interface. In the angular interrogation technique, the wavelength of the light is kept fixed and the angle of incidence is varied to fulfil the phase matching criteria. In both of these methods, once the wave vector of the incident light matches that of the SPs a resonant excitation of photon-electron coupling takes place which remains confined at the interface and decays exponentially in the transverse directions. One of the most important conditions for the excitation of SPR is that of the incident light to be in the transverse magnetic (TM)-polarization state [4–6].

Since metals have negative permittivities, usually SPRs are realised at metal-dielectric interface. But the direct incidence of TM polarized light, because of its relatively small wave vector, cannot excite SPR at the metal-dielectric interface. A high refractive index (RI) dielectric is required to transfer the extra momentum to the incident light to fulfil the wave vector matching criteria. Usually, high-k (wave vector) prism, grating, corrugated surfaces and fibers are used as a mean to supplement the extra momentum to the incident light. Prisms, being bulky, are not usually preferred.

Traditionally, noble metals such as gold (Au) and silver (Ag) are used as negative permittivity material in SPR geometry. But there are a few drawbacks of using these metals such as Ag is chemically unstable, a very thin layer of Au agglomerates and cannot form a thin uniform film [7,8]. These metals show their SPR sensitivity in the UV region of the electromagnetic spectrum and form an alloy when deposited on the top of other materials leading to different optical and electronic properties.

(a) E-mail: iitd.akhilesh@gmail.com

Furthermore, band-to-band transitions in a visible region in noble metals limit the spectral range of the applicability of the Drude free-electron model. To circumvent the issue of chemical instability, usually a thin layer of some other less reactive materials such as silicon and graphene is used over noble metals. Still the issue of the non-uniform film and absence of a visible response remains unattended.

Considering these all, conducting metal oxides (CMOs) are introduced as a replacement for these noble metals. They exhibit very smart qualities like absence of band-to-band transition, response in visible range, chemically stable, formation of very uniform thin films, etc. One of the most widely studied CMO is indium tin oxide (ITO) [9–11]. ITO is a transparent material in the UV and visible region of the spectrum and has been found to possess such characteristics for which it can support SPW at ITO-dielectric interface [9].

In the present work, a SPR-based fiber optic sensing probe has been proposed with a very large sensitivity and figure of merit (FoM) in the infrared region of the electromagnetic spectrum. The probe is designed by depositing ITO on the fiber core which is then followed by the deposition of the TiO_2 and then field enhancing silicon layers. Silicon not only protects the inner layers but also increases the sensitivity of the probe [12]. Titanium dioxide (TiO_2) is one of the most widely used semiconductors in photocatalysis and solar energy conversion. As a SPR-sensitive material, it has distinguished advantages such as low cost, high stability, high permittivity and environmental friendliness [13,14]. The thicknesses of different layers are optimized to enhance the sensitivity and FoM for the refractive index (RI) range of 1.33 to 1.37 RIU.

The model. – To experimentally realize the proposed probe, a highly multimoded plastic clad fiber is taken with core diameter of 400 μm and numerical aperture of 0.22. Cladding from the 1 cm section of the fiber is removed and this unclad portion of the fiber is coated with ITO and then with TiO_2 films which is followed by the deposition of silicon. A sensing medium is kept in contact with the topmost layer, *i.e.* with silicon. We would like to point out that the chosen diameter, radius and the length of the unclad portion of the multimode fiber are quite realistic and any variation in the diameter of the fiber or in the length of the unclad portion of the fiber will change the sensing area of the probe. These changes will only affect the coupling efficiency to the surface plasmons and the transmission spectrum will, qualitatively, remain the same. The sensor design is very simple and relatively easy to implement experimentally as compared to other fiber-based sensors such photonic-crystal-fiber–based sensors, long-period-grating–based fiber sensors and Bragg-fiber–based sensors. The schematic of the fiber probe is shown in fig. 1. To excite the SPs a polychromatic light from one end of the fiber is launched and from the other end transmission spectra are recorded. Under the condition of phase matching, the light gets coupled to the SP mode and there

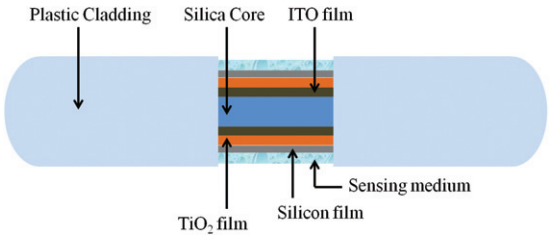

Fig. 1: (Colour on-line) Schematic of the SPR setup.

appears a dip in the transmission spectra. When the RI of the sample, in contact with the probe, is changed, a corresponding change in the position of the dip in the transmission spectrum is observed at the fiber output. The measure of this shift in the units of the wavelength gives the information about the change in the RI of the sensing medium. The N-layer matrix method has been used to numerically model the structure [15].

The characteristic matrix of the N-layer structure can be expressed as

$$M = \prod_{k=2}^{N} M_k = \begin{bmatrix} M_{11} & M_{12} \\ M_{21} & M_{22} \end{bmatrix} = \begin{bmatrix} \cos\beta_k & -i\sin\beta_k/q_k \\ -iq_k\sin\beta_k & \cos\beta_k \end{bmatrix}, \tag{1}$$

where β_k and q_k are expressed as $(2\pi d_k/\lambda)(\varepsilon_k - n_1^2\sin^2\theta_1)^{1/2}$ and $(\varepsilon_k - n_1^2\sin^2\theta_1)^{1/2}/\varepsilon_k$, respectively. d_k, n_k and ε_k are, respectively, thickness, refractive index and dielectric constant of the k-th layer in the multilayer structure. From eq. (1), we obtained the reflection coefficient r_p of the p-polarized (TM-polarized) incident wave through the stack of different layers as follows:

$$r_p = \frac{(M_{11} + M_{12}q_N)q_1 - (M_{21} + M_{22}q_N)}{(M_{11} + M_{12}q_N)q_1 + (M_{21} + M_{22}q_N)} \tag{2}$$

and the reflectance, R_p, for the p-polarized wave is

$$R_p = |r_p|^2 . \tag{3}$$

The range of angles which will lead to the guidance of the launched rays in terms of angle with the normal to the core-cladding interface can be given as follows from $\theta_1 = \sin^{-1}(n_{cl}/n_1)$ to $\theta_2 = \pi/2$, where n_1 and n_{cl} are the refractive indices of the core and the cladding of the fiber, respectively. The transmitted power at the output end of the fiber is given by

$$P_{trans} = \frac{\int_{\theta_1}^{\theta_2} R_p^{N_{ref}(\theta)} \frac{n_1^2\sin\theta\cos\theta}{\left(1-n_1^2\cos^2\theta\right)^2}\mathrm{d}\theta}{\int_{\theta_1}^{\theta_2} \frac{n_1^2\sin\theta\cos\theta}{\left(1-n_1^2\cos^2\theta\right)^2}\mathrm{d}\theta}. \tag{4}$$

The total number of reflections which the ray undergoes in the SPR sensing region of the fiber of length L and core diameter D is

$$N_{ref}(\theta) = \frac{L}{D\ \tan\theta}. \tag{5}$$

To account for the wavelength dependences of the RI of different layers deposited over the fiber core, the following dispersion relations have been considered.

The Sellmeier relation is used to determine the wavelength dependence of the refractive index of the fiber core [15],

$$n(\lambda) = \sqrt[2]{1 + \frac{a_1\lambda^2}{\lambda^2 - b_1^2} + \frac{a_2\lambda^2}{\lambda^2 - b_2^2} + \frac{a_3\lambda^2}{\lambda^2 - b_3^2}}, \qquad (6)$$

a's and b's are the Sellmeier coefficients and λ is the wavelength in μm.

The drude dispersive model is used to calculate the dielectric constants of ITO as [9]

$$\varepsilon(\lambda) = \varepsilon_r + i\varepsilon_i = 3.8 - \frac{\lambda^2\lambda_c}{\lambda_p^2(\lambda_c + i\lambda)}, \qquad (7)$$

where λ_p is the wavelength corresponding to the bulk plasma frequency and λ_c denotes the collision wavelength and is related to the losses. ITO has $\lambda_p = 0.56497\,\mu$m and $\lambda_c = 11.21076\,\mu$m [16]. ITO exhibits two SPR-sensitive dips owing their origin to two different types of plasmons. The dip in the visible region appears because of a capacitive plasmon and is less sensitive to sensing applications while the dip in the IR region has its origin in the usual SPR and is found to be very sensitive [15].

The dispersion relation for TiO_2 is accounted for by the following relation [17]:

$$\varepsilon_{TiO_2} = 5.913 + \frac{0.2441}{\lambda^2 - 0.0843} \qquad (8)$$

and the dispersion relation for silicon is [18]

$$\begin{aligned} n(\lambda) = {} & 3.44904 + 2271.88813\ \exp(-\lambda/0.05304) \\ & + 3.39538\ \exp(-\lambda/0.30384), \end{aligned} \qquad (9)$$

where wavelength is measured in μm.

The characterization of the proposed probe has been carried out in terms of the following two most important sensing parameters: sensitivity and figure of merit (FoM). Sensitivity is defined as the ratio of the shift in the resonance wavelength to the corresponding change in the refractive index (RI) of the sensing medium. FoM, on the other hand, encompasses a delicate balance of two parameters: sensitivity and detection accuracy (DA) and is defined by the following relation:

$$\text{FoM} = \text{sensitivity}/\text{FWHM} = \text{sensitivity} * \text{DA} \qquad (10)$$

where DA is inversely proportional to the full width at half-minimum (FWHM) of the transmission dip in the output spectra [15].

Results and discussion. – In fig. 2, the transmission spectra have been shown for varying thicknesses of the ITO layer, 9 nm of the TiO_2 layer and 26 nm of the silicon layer. This, as reported earlier, clearly depicts that ITO has two representative SPR-sensitive dips. These dips become prominent and get separated for high thicknesses of ITO. Furthermore, the IR dip is more sensitive to the SPR activity as compared to that of lower wavelength dip. This, therefore, encouraged us to analyze the probe with respect to the IR dip in the transmission spectrum. To determine FWHM of the second dip, it has been assumed that the second dip starts from the maximum between the two dips as shown in fig. 2(b). Put it another way, the spectrometer has working wavelength limits lying completely in the near and mid IR domain of the electromagnetic spectrum.

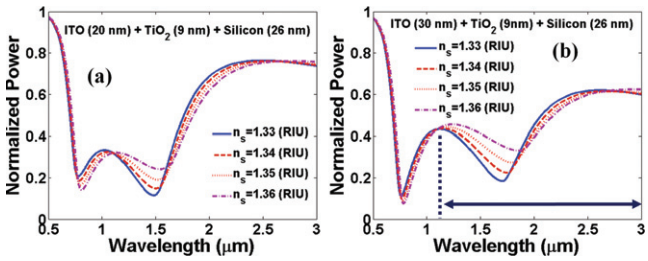

Fig. 2: (Colour on-line) Transmission (SPR) spectra at the fiber output for (a) 0.020 μm and (b) 0.030 μm of the ITO with optimized other layer thickness. The dashed vertical line is at maxima between two dips. The horizontal arrow shows the region of the second dip.

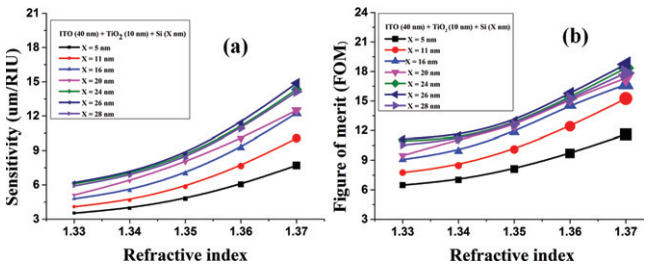

Fig. 3: (Colour on-line) (a) Sensitivity and (b) FoM plots for probe with 0.040 μm of ITO, 0.010 μm of TiO_2 and varying thickness of silicon.

Figures 3(a) and (b) show, respectively, the sensitivity and the FoM variation with sensing medium RI for the probe with 40 nm of ITO, 10 nm of TiO_2 and varying thicknesses of the silicon layer. Figure 3(a) reveals that with increasing thickness of the silicon, the sensitivity increases and it attains a maximum value for 26 nm silicon and thereafter it starts to decrease. Such trend is also shown in fig. 3(b) for FoM. Also, the sensitivity and the FoM increase with increasing sensing medium RI. In the given RI range, the largest value of the sensitivity is found to be 15.070 μm/RIU and the corresponding optimized thickness for the silicon layer is 26 nm.

To optimize the thickness of the TiO_2 layer, the ITO and silicon layers thicknesses are fixed, respectively, at 40 nm and 26 nm. The TiO_2 layer thickness is then varied to observe the sensitivity and the FoM variation with RI, as

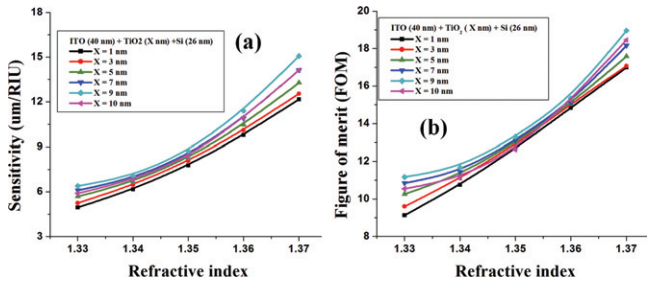

Fig. 4: (Colour on-line) (a) Sensitivity and (b) FoM plots for probe with 0.040 μm of ITO, varying thickness of TiO_2 and 0.026 μm of silicon.

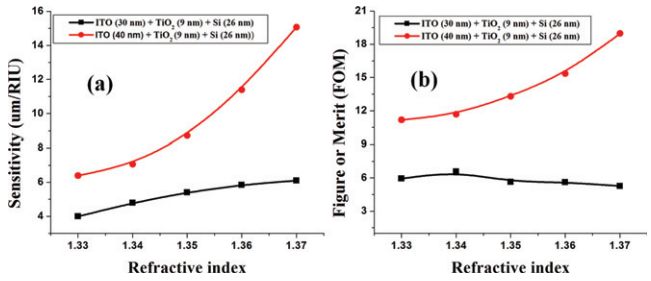

Fig. 5: (Colour on-line) (a) Sensitivity and (b) FoM plots for probe with varying thickness of ITO, 0.009 μm of TiO_2 and 0.026 μm of silicon.

shown in figs. 4(a) and (b), respectively. These figures show that the optimum TiO_2 thickness is 9 nm and also decipher the role of the thin film of the TiO_2 layer in the sensitivity enhancement.

Further, figs. 5(a) and (b) show the effects of the variation of the ITO thickness over sensitivity and FoM with other layers' thicknesses optimized. It is observed that both the parameters attain their maximum for 40 nm of ITO. Also, at 40 nm of ITO, the proposed probe works better for large sensing medium RI. Note that for probe with ITO thickness greater than 40 nm, the right arm of the transmission curve rises very little above the transmission minimum and, therefore, FWHM and thereby DA and FoM cannot be defined. Hence larger thicknesses of ITO have been ignored.

In fig. 6, SPR spectra for optimized probe design are shown for varying RI of the sensing medium. Two distinct dips are quite evident. The sensitivity of the visible dip (capacitive SPR dip) is quite low as compared to that of the IR dip (usual SPR dip).

Thus, the optimized probe parameters are 40 nm ITO, 9 nm TiO_2 and 26 nm of silicon and the maximum values of the sensitivity and FoM are 15.070 μm/RIU and 18.962 RIU^{-1} respectively. The values of the maximum sensitivities and FoMs in different probe designs discussed in figs. 3, 4 and 5 are given in table 1.

The sensitivity of the proposed probe is much higher than the earlier reported results such as 5 μm/RIU in SPR-based tapered fiber-optic sensor [19], 0.032 μm/RIU in multimode interference-based photonic crystal fiber [20]

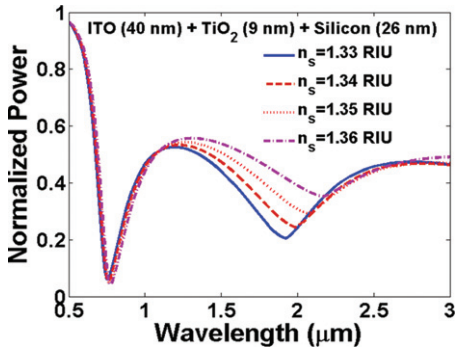

Fig. 6: (Colour on-line) Transmission (SPR) spectra at the fiber output for the proposed probe with optimized parameters, *i.e.* 0.040 μm of ITO, 0.009 μm of TiO_2 and 0.026 μm of silicon.

Table 1: Values of the maximum sensitivities and FoMs in different probe designs discussed in figs. 3, 4 and 5.

Figure	3(a)	4(a)	5(a)
Sensitivity @ 1.37 RIU (μm/RIU)	14.870	15.070	15.070
Figure	3(b)	4(b)	5(b)
Figure of Merit @ 1.37 RIU (1/RIU)	18.112	18.962	18.962

and recently reported 5.7 μm/RIU in D-shaped fiber sensor [21].

The proposed probe is chemically stable, being fiber based, is immune to electromagnetic interferences and is, therefore, advantageous over resistive sensors. In addition, online monitoring and miniaturization put such sensors atop of the SPR-based prism sensors.

Conclusion. – A theoretical study has been carried out to characterize an extremely sensitive SPR-based fiber optic sensing probe working in the IR region of the electromagnetic spectrum. The sensing probe comprises ITO, TiO_2 and silicon layers on the fiber core. The characterization has been performed in terms of two important sensing parameters: sensitivity and FoM. The maximum values of sensitivity and FoM are found to be 15.070 μm/RIU and 18.962 RIU^{-1}, respectively.

* * *

One of the authors, AKM, acknowledges support in part at the Technion by a fellowship of the Israel Council for Higher Education.

REFERENCES

[1] Mühlschlegel P. *et al.*, *Science*, **308** (2005) 1607.
[2] Shalaev V. M. *et al.*, *Opt. Lett.*, **30** (2005) 3356.
[3] Kumar A. and Mishra A. K., *J. Opt. Soc. Am. B*, **29** (2012) 1330.

[4] Caucheteur C. *et al.*, *Anal. Bioanal. Chem.*, **407** (2015) 3883.
[5] Mishra A. K. *et al.*, *Plasmonics*, **10** (2015) 1071.
[6] Mishra S. K., Kumari D. and Gupta B. D., *Sens. Actuators B: Chem.*, **171-172** (2012) 976.
[7] Rhodes C. *et al.*, *J. Appl. Phys.*, **103** (2008) 093108.
[8] Kanso M. *et al.*, *J. Opt. A: Pure Appl. Opt.*, **9** (2007) 586.
[9] Franzen S., *J. Phys. Chem. C*, **112** (2008) 6027.
[10] Franzen S. *et al.*, *Opt. Lett.*, **34** (2009) 2867.
[11] Zamarreño C. R. *et al.*, *Sens. Actuators B: Chem.*, **146** (2010) 414.
[12] Shalabney A. and Abdulhalim I., *Sens. Actuators A: Phys.*, **159** (2010) 24.
[13] Hernáez M. *et al.*, *Appl. Opt.*, **49** (2010) 3980.
[14] Paliwal N. and John J., *Appl. Opt.*, **53** (2014) 3241.
[15] Mishra A. K. *et al.*, *Opt. Commun.*, **344** (2015) 86.
[16] Verma R. K. and Gupta B. D., *J. Opt. Soc. Am. A*, **27** (2010) 846.
[17] DeVore J. R., *J. Opt. Soc. Am.*, **41** (1951) 416.
[18] Bhatia P. and Gupta B. D., *Appl. Opt.*, **50** (2011) 2032.
[19] Díaz-Herrera N. *et al.*, *Sens. Actuators B: Chem.*, **146** (2010) 195.
[20] Coelho L. *et al.*, *Microwave Opt. Technol. Lett.*, **54** (2012) 1009.
[21] Patnaik A., Senthilanathan K. and Jha R., *IEEE Photon. Technol. Lett.*, **27** (2015) 2437.